

Title: CMB Beyond Planck

Date: Oct 30, 2018 11:00 AM

URL: <http://pirsa.org/18100045>

Abstract:

In July 2018 the Planck Collaboration released its final set of cosmology results. I will discuss some of the interesting new science that remains to be done with the CMB, including some not so often discussed topics such as the kinetic SZ effect and 21cm cross-correlations.

The CMB Beyond Planck

Martin Bucher
Université Paris 7/CNRS, Paris, France
and
University of KwaZulu-Natal, Durban, South Africa

30 October 2018, Perimeter Institute, Waterloo, Ontario, Canada

Talk Outline



1. Planck Legacy (focusing mainly on primordial aspects)
2. Current high- ℓ observations from the ground (largely exploring the so-called secondary anisotropies, of which we choose the kSZ as an example)
3. Correlation with 21cm, challenges for 21cm intensity mapping

2018 Planck Legacy Release

<https://www.cosmos.esa.int/web/planck/publications>



SCIENCE MISSIONS

EUROPEAN SPACE AGENCY

SCIENCE & TECHNOLOGY

planck

esa

Planck - Publications

Home

Mission Overview

Mission History

Planck Legacy Archive

Publications

Poster Gallery

Conferences

Planck Teams

Reprocessed Planck Data

Lessons Learned

PLANCK PUBLICATIONS

On this page you can find a list of Planck publications, ordered as follows:

- Papers by the [Planck Collaboration](#), categorized into groups:
 - Planck 2018 results. [Planck 2018 results I: Low Frequency Instrument data processing](#)
 - Planck 2018 results. [Planck 2018 results II: High Frequency Instrument data processing and frequency maps](#)
 - Planck 2018 results. [Planck 2018 results III: Cosmological parameters](#)
 - Planck 2018 results. [Planck 2018 results IV: Cosmological lensing](#)
 - Planck 2018 results. [Planck 2018 results V: Cosmological magnetics](#)
 - Planck 2018 results. [Planck 2018 results VI: Cosmological magnetics using polarized dust emission](#)
- Papers using Planck data that are not authored by the [Planck Collaboration](#) are collected separately into an ADS query [here](#).
- A compilation of all the papers the [Planck Collaboration](#) and by other authors is collected into an ADS query [here](#).
- The Planck data used to set standards and conventions for Planck papers, is [here](#).
- The Planck bibliography references list in [BIBPlanck](#) [here](#).
- [Errata](#) (papers corrected to Planck or fixed text).
- A report on [Planck corrections](#) issued in May 2018. If you have any feedback or further questions on any of the topics discussed in this document, please contact [planck_publications@esa.int](#).

PLANCK 2018 RESULTS

The first release of the 2018 PLANCK results using the full mission data are presented here. These results are produced by the [Planck Collaboration](#). The papers are available online, and links to each are provided below. If you use any of these results for presentations, please acknowledge the corresponding paper, [BIBPlanck](#), and the Planck Collaboration. The Planck Legacy Archive (PLA) contains all public products originating from the Planck mission.

Title	Authors	Publication
Planck 2018 results. I. Overview and the cosmological legacy of Planck	Planck Collaboration	Submitted to A&A
Planck 2018 results. II. Low Frequency Instrument data processing	Planck Collaboration	Submitted to A&A
Planck 2018 results. III. High Frequency Instrument data processing and frequency maps	Planck Collaboration	Accepted by A&A
Planck 2018 results. IV. Cosmological parameters	Planck Collaboration	Submitted to A&A
Planck 2018 results. V. Cosmological lensing	Planck Collaboration	Submitted to A&A
Planck 2018 results. VI. Cosmological magnetics	Planck Collaboration	Submitted to A&A
Planck 2018 results. VII. Cosmological magnetics using polarized dust emission	Planck Collaboration	Submitted to A&A

PLANCK 2015 RESULTS

The first release of the 2015 PLANCK results using the full mission data are presented here. These results are produced by the [Planck Collaboration](#). The papers are available online, and links to each are provided below. If you use any of these results for presentations, please acknowledge the corresponding paper, [BIBPlanck](#), and the Planck Collaboration. The Planck Legacy Archive (PLA) contains all public products originating from the Planck mission.

Title	Authors	Publication
Planck 2015 results. I. Overview of products and results	Planck Collaboration	2016, A&A, 596, A1

COSMOLOGY

2018 Gruber Cosmology Prize Citation

The Gruber Foundation is pleased to present the 2018 Cosmology Prize to the Planck Team, and to Jean-Loup Puget and Nazareno Mandolese, the leaders of the HFI and LFI instrument consortia, for mapping the temperature and polarization of the cosmic microwave background radiation with the ESA Planck spacecraft.

Planck measured, with unprecedented precision, the matter content and geometry of the universe, the imprint on the CMB of hot gas in galaxy clusters and of gravitational lensing by large-scale structure, constrained a hypothetical inflationary phase, probed down when the first stars formed, and provided unique information about interstellar dust and magnetic fields in our Galaxy.

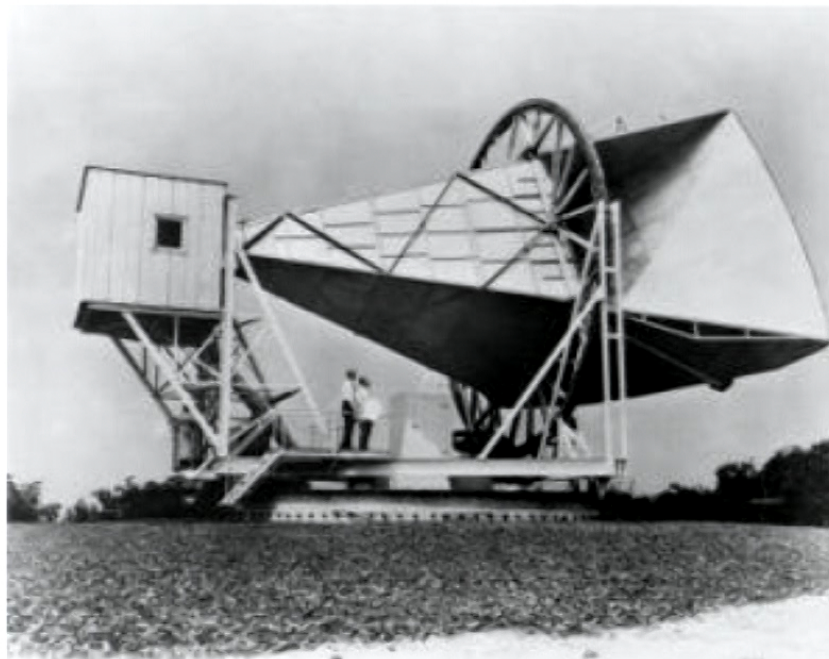
[See Gruber Lecture slides of Reno Mandolesi and Jean-Loup Puget from Tuesday for more details on Planck 2018 Results]

Pirsa: 18100045

Page 4/38

Discovery of the cosmic microwave background

1963 Penzias and Wilson (Bell Labs) observed a background of microwaves having a thermal spectrum with $T = 2.753K$. This temperature is (almost) the same no matter what the direction in the sky.



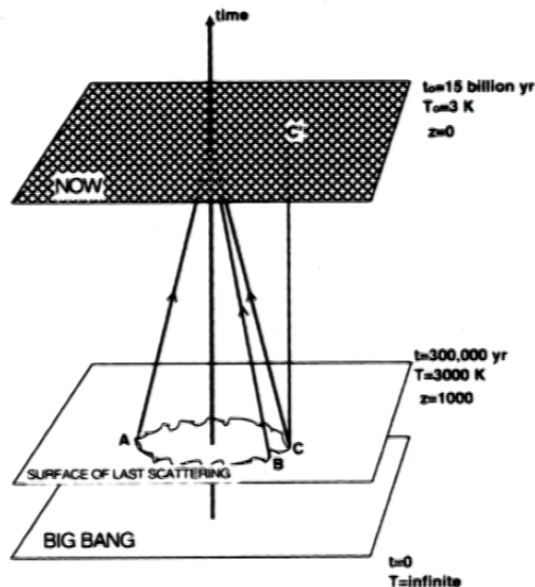
Theory – origin of the CMB anisotropy

Sachs-Wolfe formula

$$\frac{\delta T}{T}(\hat{\mathbf{n}}) = \left[\frac{1}{4}\delta_\gamma + \mathbf{v}_\gamma \cdot \mathbf{n} + \Phi \right]_i^f + 2 \int_i^f d\eta \frac{\partial \Phi'}{\partial \eta}(\eta, \hat{\mathbf{n}}(\eta_0 - \eta))$$

$\Phi \equiv$ Newtonian gravitational potential (dimensionless)

δ_γ and \mathbf{v}_γ describe the fractional density contrast and peculiar 3-velocity of the photon component.



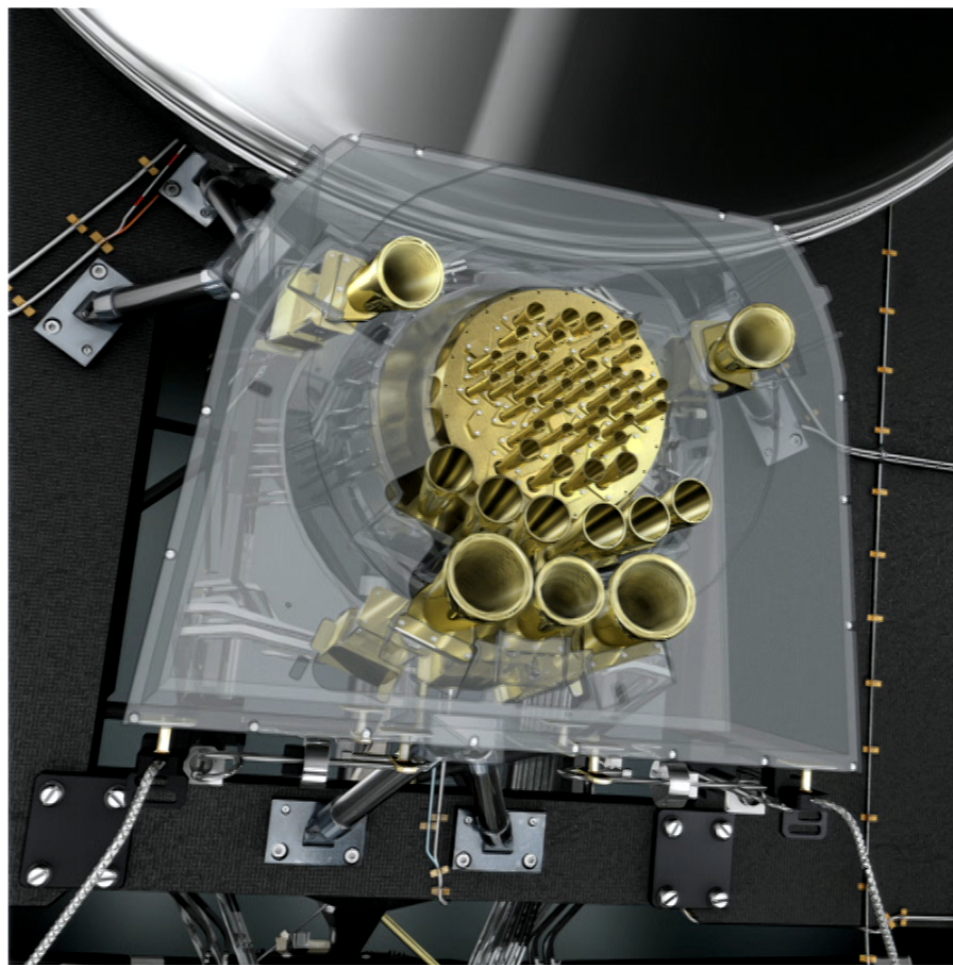
This treatment is somewhat naive because it assumes that the surface of last scatter is infinitely thin.

In reality the surface of last scatter has a width that smears the anisotropies on small scales.

The *Planck* mission



PLANCK Focal Plane



T & P Signals vs Frequency

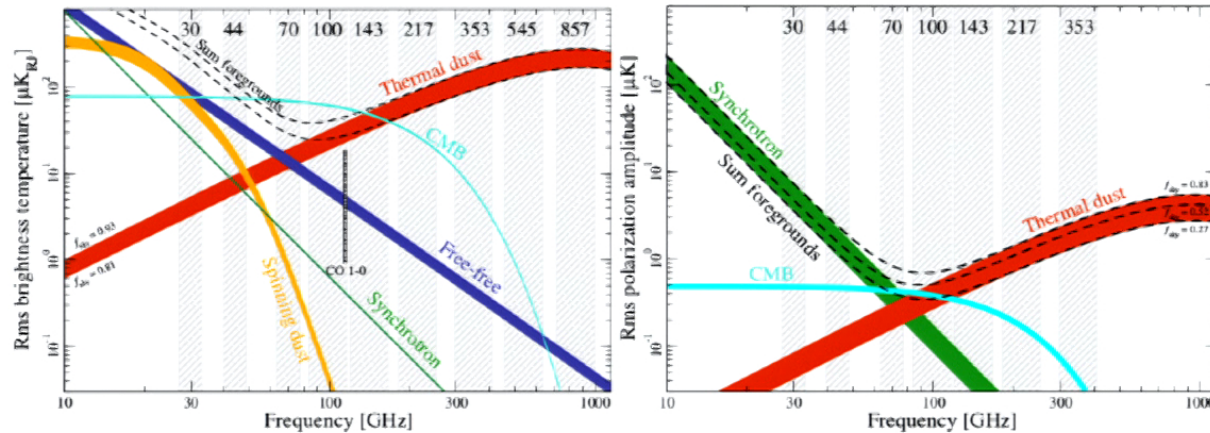
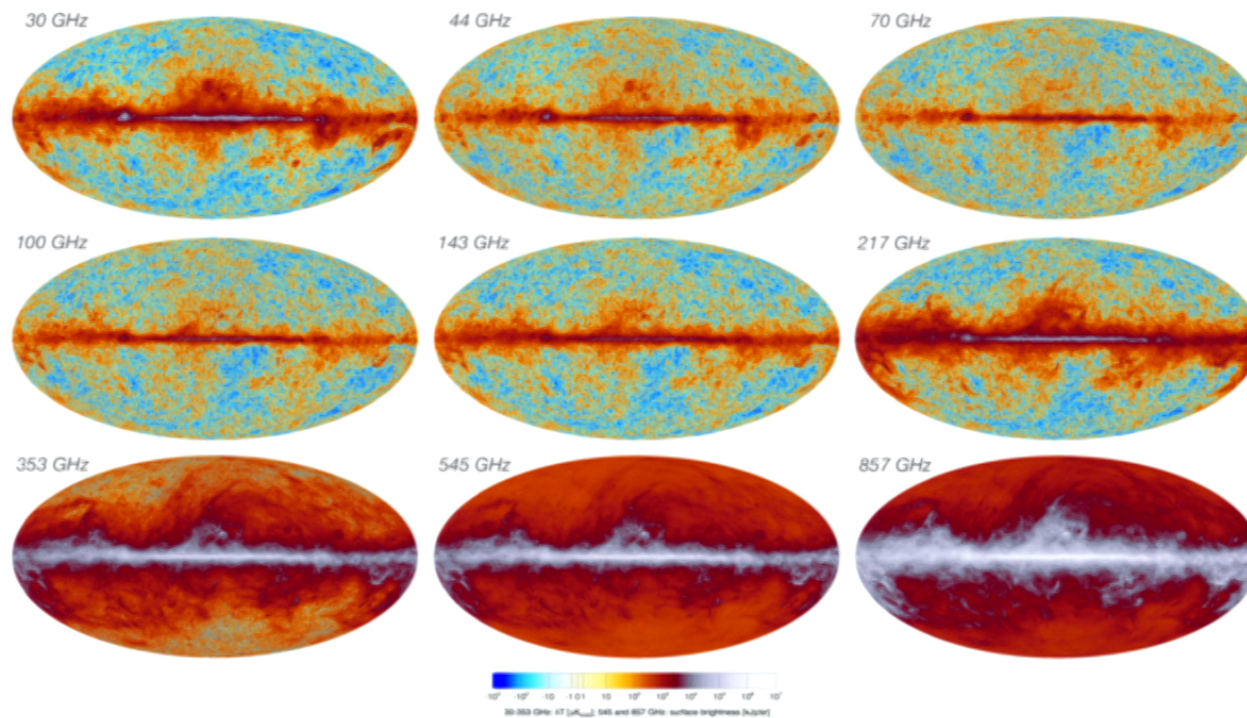
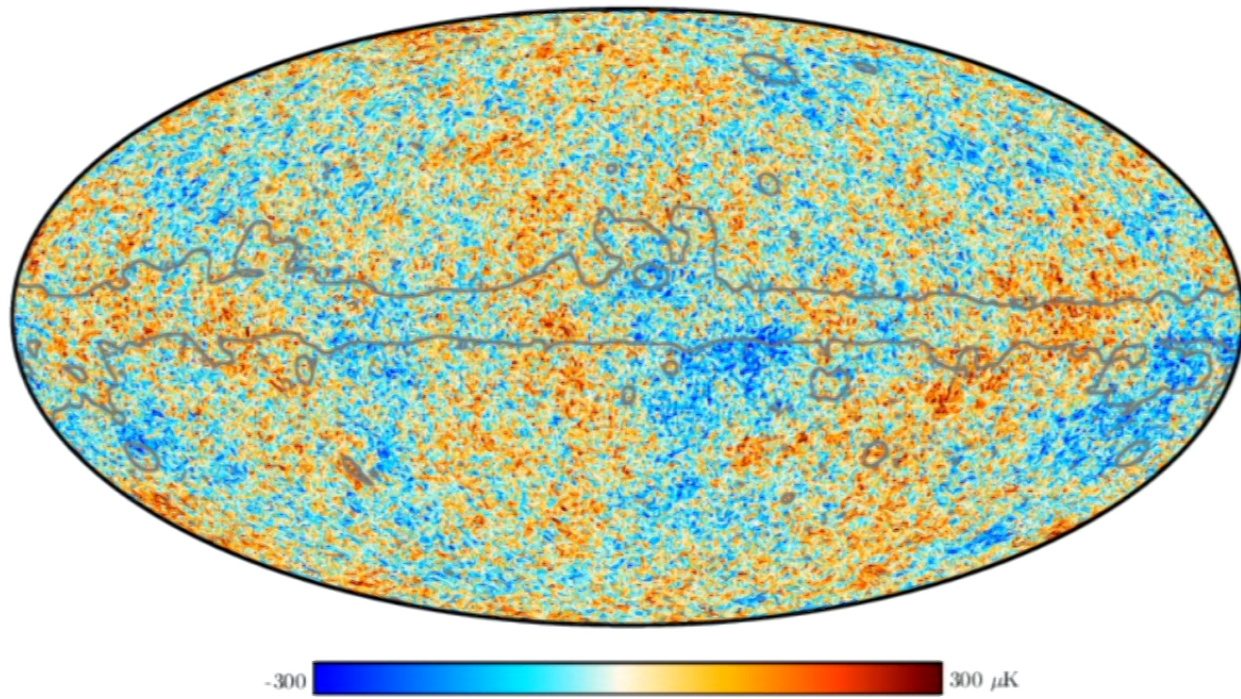


Fig. 4. Frequency dependence of the main components of the submillimetre sky in temperature (left) and polarization (right). The (vertical) grey bands show the *Planck* channels, with the coloured bands indicating the major signal and foreground components. For temperature the components are smoothed to 1° and the widths of the bands show the range for masks with 81–93 % sky coverage. For polarization the smoothing is $40'$ and the range is 73–93 %. Note that for steep spectra, the *rms* shown here is dominated by the largest angular scales. But as shown by Fig. 5, on much smaller angular scales in regions far from the Galactic plane, the foreground signals fall far below the cosmological signal (except at the lowest ℓ , in polarization).

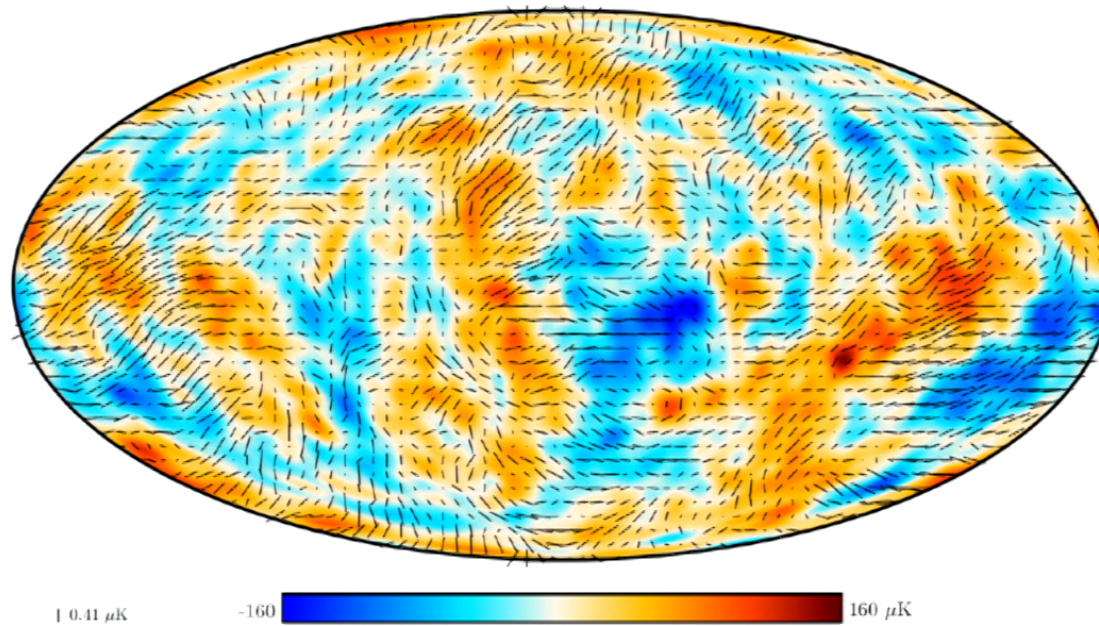
Planck Raw Temperature Maps



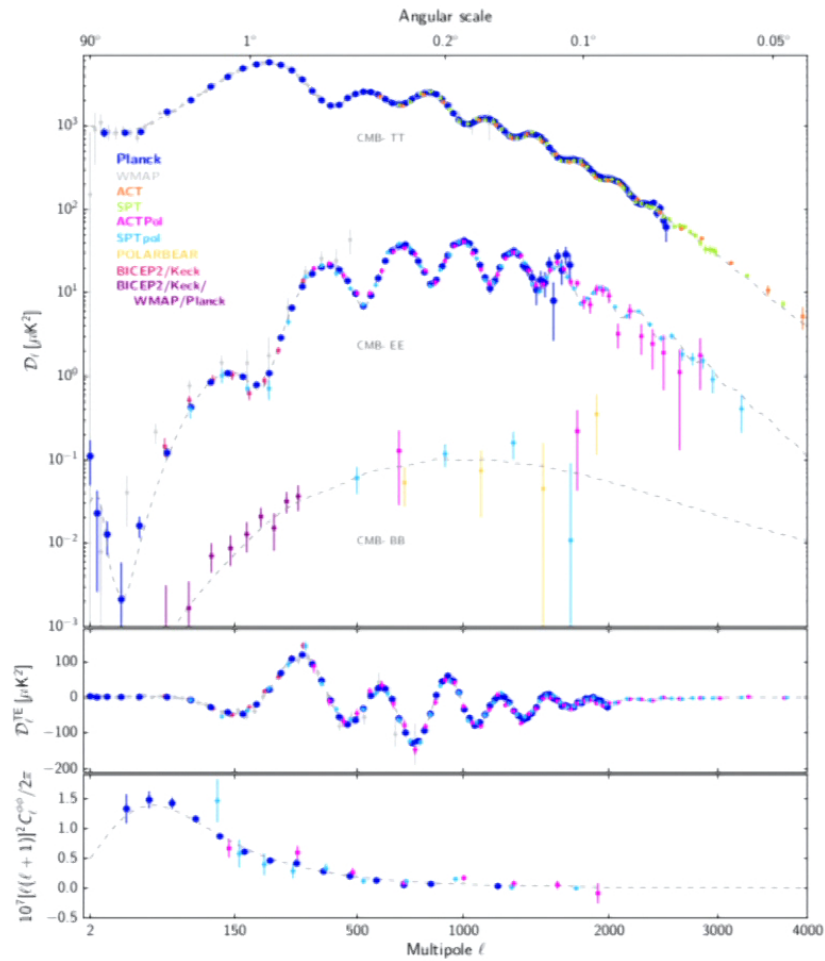
Cleaned Temperature Map



Cleaned Polarization Map



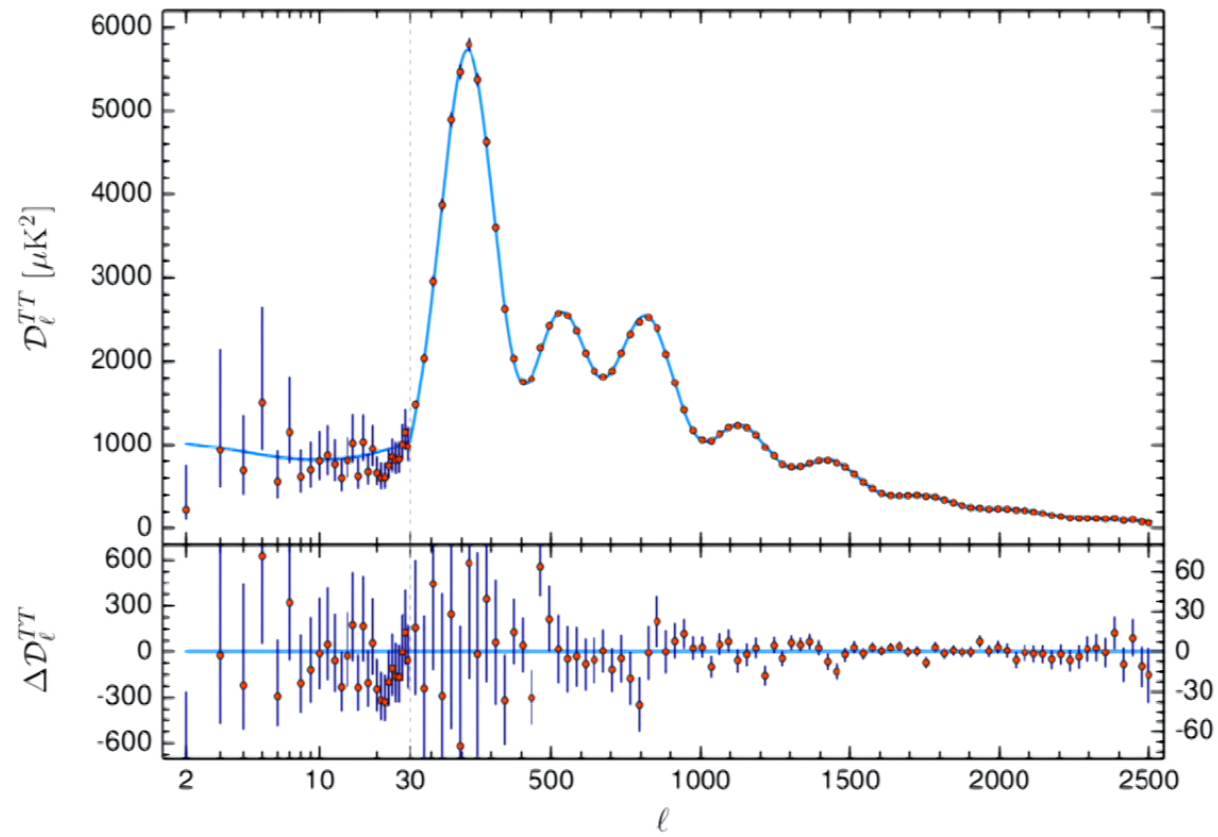
CMB Power Spectra: Current State of the Art



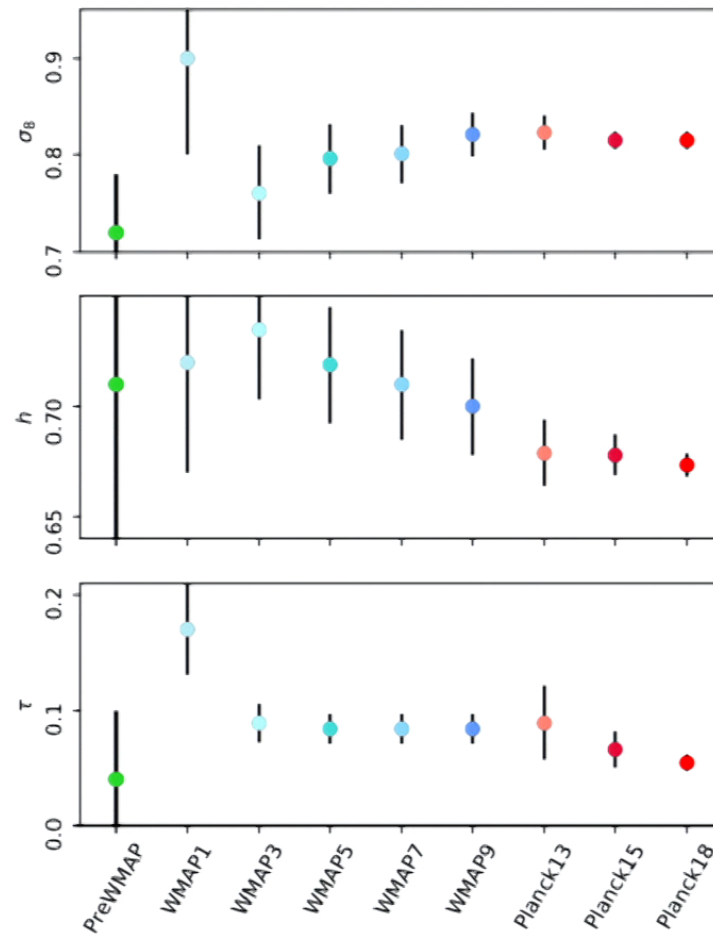
Parameters of the 6-Parameter Concordance Model

Parameter	Plk best fit	Plk [1]	CamSpec [2]	$([2] - [1])/\sigma_1$	Combined
$\Omega_b h^2$	0.022383	0.02237 ± 0.00015	0.02229 ± 0.00015	-0.5	0.02233 ± 0.00015
$\Omega_c h^2$	0.12011	0.1200 ± 0.0012	0.1197 ± 0.0012	-0.3	0.1198 ± 0.0012
$100\theta_{MC}$	1.040909	1.04092 ± 0.00031	1.04087 ± 0.00031	-0.2	1.04089 ± 0.00031
τ	0.0543	0.0544 ± 0.0073	$0.0536^{+0.0069}_{-0.0077}$	-0.1	0.0540 ± 0.0074
$\ln(10^{10} A_s)$	3.0448	3.044 ± 0.014	3.041 ± 0.015	-0.3	3.043 ± 0.014
n_s	0.96605	0.9649 ± 0.0042	0.9656 ± 0.0042	+0.2	0.9652 ± 0.0042
$\Omega_m h^2$	0.14314	0.1430 ± 0.0011	0.1426 ± 0.0011	-0.3	0.1428 ± 0.0011
H_0 [km s ⁻¹ Mpc ⁻¹] . . .	67.32	67.36 ± 0.54	67.39 ± 0.54	+0.1	67.37 ± 0.54
Ω_m	0.3158	0.3153 ± 0.0073	0.3142 ± 0.0074	-0.2	0.3147 ± 0.0074
Age [Gyr]	13.7971	13.797 ± 0.023	13.805 ± 0.023	+0.4	13.801 ± 0.024
σ_8	0.8120	0.8111 ± 0.0060	0.8091 ± 0.0060	-0.3	0.8101 ± 0.0061
$S_8 \equiv \sigma_8(\Omega_m/0.3)^{0.5}$. .	0.8331	0.832 ± 0.013	0.828 ± 0.013	-0.3	0.830 ± 0.013
z_{re}	7.68	7.67 ± 0.73	7.61 ± 0.75	-0.1	7.64 ± 0.74
$100\theta_*$	1.041085	1.04110 ± 0.00031	1.04106 ± 0.00031	-0.1	1.04108 ± 0.00031
r_{drag} [Mpc]	147.049	147.09 ± 0.26	147.26 ± 0.28	+0.6	147.18 ± 0.29

Planck 2018 TT With Residuals



Evolution of Cosmological Parameters



Inflationary Models: n_s - r Plane

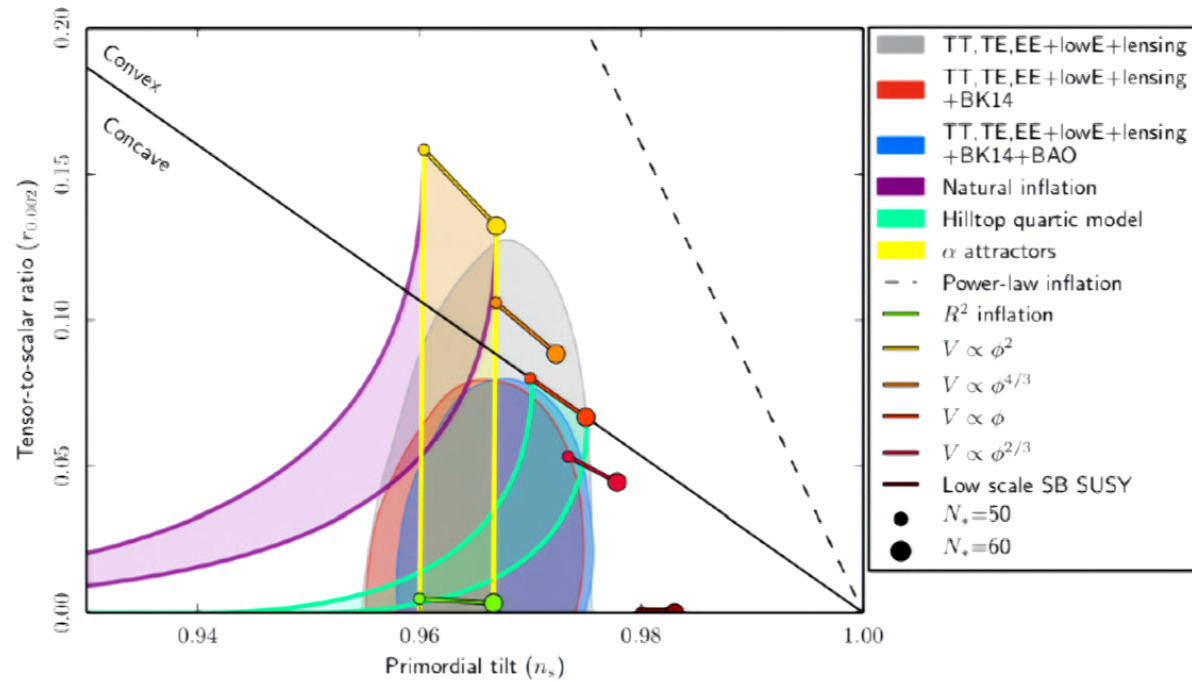
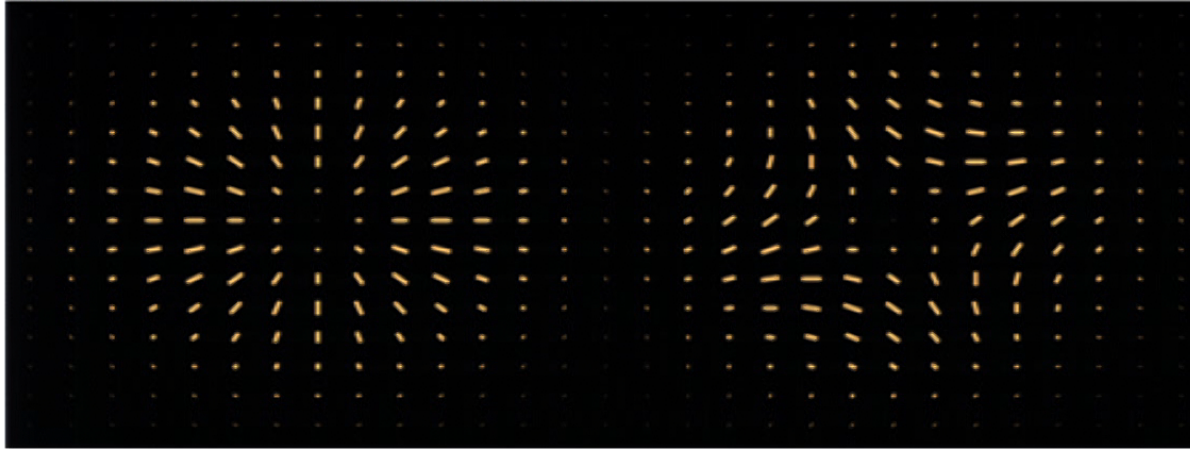


Fig. 23. Limits on the tensor-to-scalar ratio, $r_{0.002}$ as a function of n_s in the Λ CDM model at 95% CL, from *Planck* alone (grey area) or including BICEP2/Keck data 2014 (red) and BAO (blue). Constraints assume negligible running of the inflationary consistency relation and the lines show the predictions of a number of models as a function of the number of e -folds, N_* , till the end of inflation. This can be compared with the middle panel in the top row of Fig. 14 which gives a temporal perspective.

Concordance Scorecard

Prediction	Measurement
A spatially flat universe	$\Omega_K = 0.0007 \pm 0.0019$
with a <i>nearly</i> scale-invariant (red)	
spectrum of density perturbations,	$n_s = 0.967 \pm 0.004$
which is almost a power law,	$dn/d \ln k = -0.0042 \pm 0.0067$
dominated by scalar perturbations,	$r_{0.002} < 0.07$
which are Gaussian	$f_{\text{NL}} = 2.5 \pm 5.7$
and adiabatic,	$\alpha_{-1} = 0.00013 \pm 0.00037$
with negligible topological defects	$f < 0.01$

E and B Mode Polarization



E mode

B mode

$$\mathbf{Y}_{\ell m, ab}^{(E)} = \sqrt{\frac{2}{(\ell-1)\ell(\ell+1)(\ell+2)}} \left[\nabla_a \nabla_b - \frac{1}{2} \delta_{ab} \nabla^2 \right] Y_{\ell m}(\hat{\Omega})$$

$$\mathbf{Y}_{\ell m, ab}^{(B)} = \sqrt{\frac{2}{(\ell-1)\ell(\ell+1)(\ell+2)}} \frac{1}{2} \left[\epsilon_{ac} \nabla_c \nabla_b + \nabla_a \epsilon_{bc} \nabla_c \right] Y_{\ell m}(\hat{\Omega})$$

Secondary CMB Anisotropies

After subtraction of the CMB monopole and dipole, $\frac{\delta T}{T}$ for $\ell \lesssim 3000$ is dominated by the **primary** CMB anisotropies, which emanate from the **surface of last scatter** (i.e., almost at past intersection of our past light cone with the putative big bang singularity).

However, there are also other **secondary** anisotropies, which are imprinted as the photons propagate from the surface of last scatter to us today. ¹ These include:

1. Gravitational Lensing of the CMB by intervening structures at intermediate redshift.
2. The Thermal Sunyaev-Zeldovich (tSZ) Effect
3. The Kinetic (or Kinematical) Sunyaev-Zeldovich (kSZ) Effect

¹However, the integrated Sachs-Wolfe effect, the effect of rescattering by homogeneous reionization (i.e., τ) are conventionally regarded as being 'primary' anisotropies.

The Sunyaev-Zeldovich Effects

- ▶ Consider the rescattering of the CMB monopole by a cloud of possibly very hot reionized gas (e.g., from the diffuse ionized gas in a cluster).
- ▶ If the cloud had no peculiar motion (w.r.t. the Hubble flow) and if the electron gas temperature is exactly equal to the CMB temperature, the net effect is null, as if the cloud were not there.

- ▶ But,

- ▶ kSZ: If the cloud is moving w.r.t. the local CMB rest frame, a dipole contribution

$$\frac{\delta T}{T_0}_{kSZ} = \frac{\tau}{c} (\hat{\mathbf{n}} \cdot \mathbf{v})$$

is superimposed on the primary anisotropies, also with a perturbed blackbody frequency spectrum.

- ▶ tSZ: If the cloud is hot $T \gg T_{CMB}$, a spectral distortion of the form

$$\left(\frac{\delta T(\nu)}{T_0} \right)_{tSZ} = \frac{\tau}{m_e c^2} F(x) = \delta y F(x)$$

where $x = \nu/\nu_{CMB}$, $\nu_{CMB} = k_B T/h$, and

$$F(x) = \frac{x(e^x + 1)}{e^x - 1} - 4$$

is superimposed.



kSZ and Peculiar Velocities

The kSZ effect is notoriously hard to measure because:

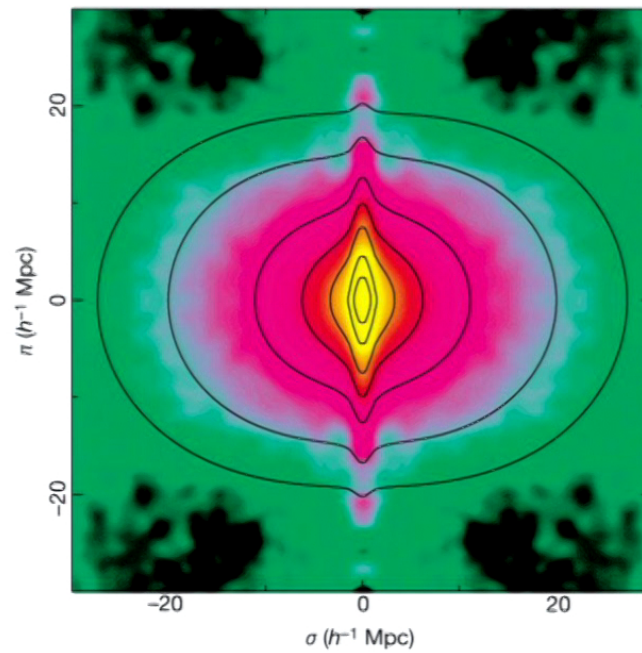
1. Unlike the tSZ effect, the kSZ has *precisely the same frequency dependence* as the primary CMB anisotropies (i.e., that of a perturbed temperature blackbody).
2. It is **much smaller** in magnitude than the primary CMB anisotropies.

Therefore, the easiest and best way to detect the kSZ is through **cross-correlations**.

One makes a prediction for δT_{kSZ} (e.g., using data from 3d galaxy surveys, possibly combined with tSZ data) and then cross correlates this template with a properly filtered and cleaned map of $\delta T_{blackbody}^{sky}$.

Aside: This is how gravitational lensing of the CMB was first detected [K. Smith, O. Zahn & O. Doré, PRD 76 (2007) 043510 3.4σ from WMAP + VLA radio galaxies], although now Planck measures CMB lensing directly, without resorting to cross-correlations. [Planck 2013 results. XVII. Gravitational lensing by large-scale structure Planck Collaboration, at 23σ]

Fingers of God vs. Pancakes of God



[John A. Peacock et al. "A measurement of the cosmological mass density from clustering in the 2dF Galaxy Redshift Survey," Nature 410 (2001) 169]

kSZ: A unique probe of peculiar velocities to arbitrarily high z

- ▶ Competing probes of peculiar velocities (i.e., using “standard candles”) have errors that increase with z and thus are useful only within a small sphere in our immediate vicinity.
- ▶ kSZ peculiar velocities instead measure velocities relative to the local CMB rest frame (in which the CMB dipole about the object vanishes). [This is not a perfect reference but better than any other empirical cosmic rest frame.] Thus the errors are roughly independent of z . Thus we can probe peculiar velocities almost anywhere within our causal horizon.

Current status of kSZ observations

There are two basic strategies:

1. Select two massive collapsed objects that should be falling toward each other and predict $\delta T(1) - \delta T(2)$ including its sign, which is random for the noise from the primary CMB anisotropies. Challenge is to filter out the primary CMB signal and also the contamination from kSZ. Use stacking to accumulate S/N .
2. Reconstruct the entire proper velocity field $\mathbf{v}(\mathbf{x})$ to make a template for the expected $\delta T(\hat{\mathbf{n}})$ and cross-correlate with $\delta T_{\text{blackbody}}^{\text{sky}}(\hat{\mathbf{n}})$ with the statistic

$$\left\langle \delta T(\hat{\mathbf{n}}) \delta T_{\text{blackbody}}^{\text{sky}}(\hat{\mathbf{n}}) \right\rangle.$$

Whereas the tSZ signal is dominated by highly collapsed objects (where the gas is especially hot) and roughly probes gas pressure along the line of sight, the kSZ probes the peculiar velocity field of the gas everywhere as long as it is ionized, or gas momentum averaged and projected along the line of sight.

Here we have emphasized proper velocity field, but the baryon density as well as the ionization fraction enters into determining the signal. Thus given a knowledge of the peculiar velocity field, we can probe where the ionized gas is situated.

First detection of kSZ

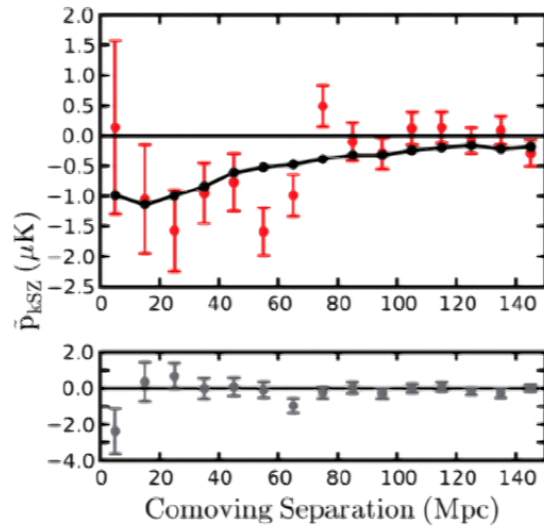


FIG. 1: The upper panel shows the mean pairwise momentum estimator, Eq. (4), for the 5000 most luminous BOSS DR9 galaxies within the ACT sky region (red points), with bootstrap errors. The solid line is derived from numerical kSZ simulations [34] using a halo mass cutoff of $M_{200} = 4.1 \times 10^{13} M_{\odot}$. The probability of the data given a null signal is 2.0×10^{-3} including bin covariances. The lower panel displays the same sum but with randomized map positions, and is consistent with a null signal.

Nick Hand et al. (ACT Collaboration),
 “Evidence of Galaxy Cluster Motions
 with the Kinematic Sunyaev-Zeldovich
 Effect,” Phys. Rev. Lett. 109 (2012)
 041101 ($\approx 2.9\sigma$ detection)

$$\tilde{p}_{\text{pair}}(r) = \frac{\sum_{i<j} (\mathbf{p}_i \cdot \hat{\mathbf{r}}_i - \mathbf{p}_j \cdot \hat{\mathbf{r}}_j) c_{ij}}{\sum_{i<j} c_{ij}^2}$$

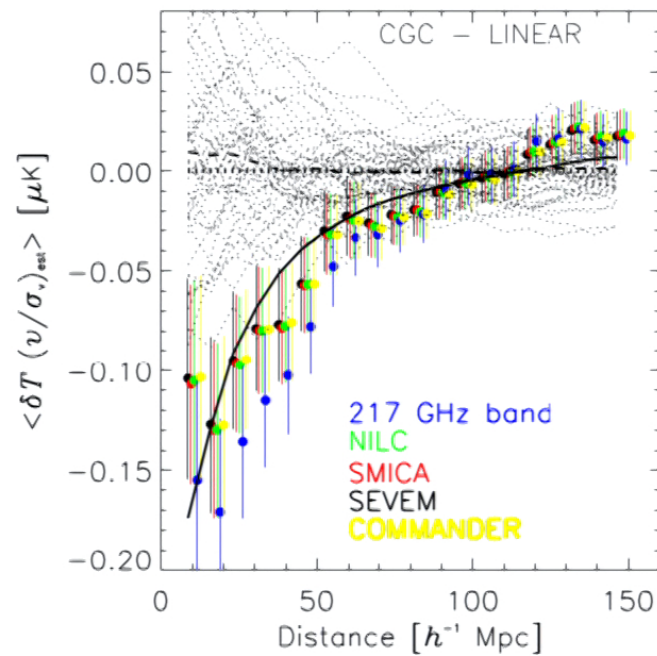
$$c_{ij} \equiv \hat{\mathbf{r}}_{ij} \cdot \frac{\hat{\mathbf{r}}_i + \hat{\mathbf{r}}_j}{2} = \frac{(r_i - r_j)(1 + \cos \theta)}{2\sqrt{r_i^2 + r_j^2 - 2r_i r_j \cos \theta}},$$

$$\tilde{p}_{\text{kSZ}}(r) = -\frac{\sum_{i<j} [(T_i - \mathcal{T}(z_i)) - (T_j - \mathcal{T}(z_j))] c_{ij}}{\sum_{i<j} c_{ij}^2}.$$

Another example

Planck Collaboration: P. A. R. Ade et al., Planck intermediate results XXXVII.

Evidence of unbound gas from the kinetic Sunyaev-Zeldovich effect A&A 586, A140
(2016)



Many other papers (e.g., SPT & DES,...)

21 cm observations as a cross-correlation candidate

(Work in progress with Zahra Kader and Kavilan Moodley)

- ▶ Intensity mapping (meaning one does not resolve and pick out individual galaxies)
- ▶ Redshift range $z=0.8-2.5$ over a large fraction of the Southern sky
- ▶ Primary science objective is to characterize the Dark Energy (with BAO) as with CHIME but in the Southern sky
- ▶ But there is also a lot of interesting cross-correlation science possible (of which X-Correl with kSZ is but one example)

$$\delta T_{sky}(\hat{\Omega}, \nu) = \delta T_{synch}(\hat{\Omega}, \nu) + \delta T_{extra-galactic}(\hat{\Omega}, \nu)$$

The much hotter parasitic contaminant from our galaxy $\delta T_{synch}(\hat{\Omega}, \nu)$ is smooth in frequency (almost a single power law in ν) [i.e., dominated by low $|k_{\parallel}|$ modes]

However, the sought after signal $\delta T_{extra-galactic}(\hat{\Omega}, \nu)$ is clumpy for all \mathbf{k}_{\perp} and k_{\parallel} .

Consequence: We must throw away the low k_{\parallel} modes, or do something more or less equivalent to that.

kSZ: The Future (Toward the CMB Stage-4 Experiment)



- ▶ Since galaxy clusters are small, kSZ studies are ideally performed by mapping the microwave sky from the ground, where telescopes of diameter 6 – 10 *m* can be deployed at a reasonable cost.
- ▶ The high resolution maps, for example from ACT and SPT, are sufficient for a proof of concept, but there is much scope for improvement in (1) the sensitivity of the maps, (2) fraction of sky covered, and (3) better frequency coverage (in order to remove kSZ as well as the more conventional foregrounds).
- ▶ Likewise, because of the importance of cross-correlations, more extensive and deeper 3d galaxy surveys promise to improve on what is currently possible.

kSZ cross-correlation with 21cm observations

$$\begin{aligned}
 \left(\begin{array}{c} \text{21cm source} \\ \text{function} \end{array} \right) &\propto (\bar{\rho} + \delta\rho)\mathbf{v} \\
 &= \underbrace{\bar{\rho}\mathbf{v}}_{\text{inaccessible with 21cm}} + \underbrace{(\delta\rho)\mathbf{v}}_{\text{21cm bispectral signal}}
 \end{aligned}$$

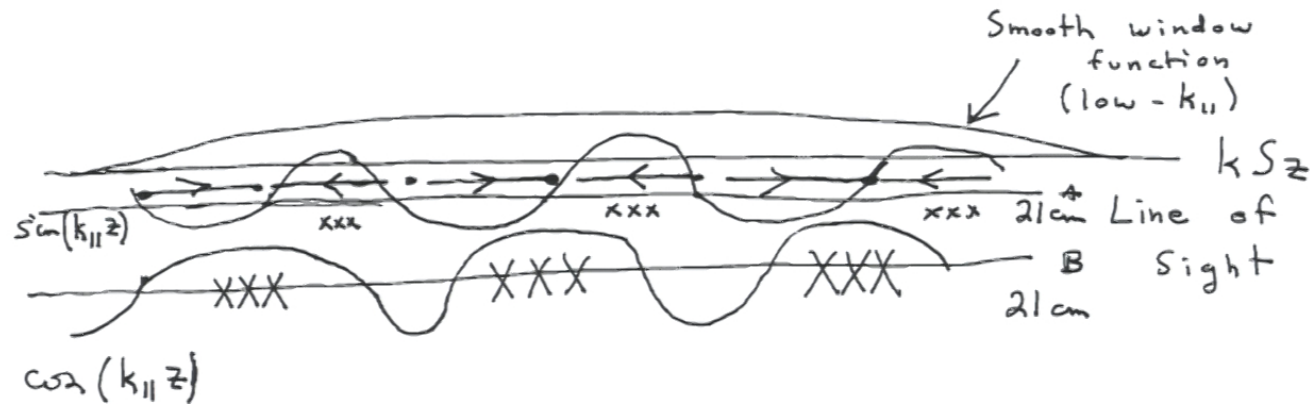
Triangle equalities (here in flat-sky approximation):

$$\mathbf{k}_{\perp,1}^{kSz} + \mathbf{k}_{\perp,2}^{21cm} + \mathbf{k}_{\perp,3}^{21cm} = 0,$$

$$0 + \mathbf{k}_{\parallel,2}^{21cm} + \mathbf{k}_{\parallel,3}^{21cm} = 0.$$

Mathematically, somewhat like bispectral non-Gaussianity in CMB maps except that there is an extra dimension: k_{\parallel} .

Bispectral Observable: $\langle \delta T_{kSz}(\hat{\Omega}_{kSz}) \delta T^{21cm}(\hat{\Omega}_{Sz}^A, \hat{p}_{11}) \delta T^{21cm}(\hat{\Omega}_{Sz}^B, -\hat{p}_{11}) \rangle$



To get a δT_{kSz} contribution, the contributions from the 21cm lines of sight must ideally lag or lead by 90° in phase. The real (0° or 180° phase) give no kSz signal.

The Hydrogen Intensity and Real-time Analysis eXperiment

Science goals:

Measure baryon acoustic oscillations with HI intensity mapping

Characterize dark energy

Radio transient searches

Pulsar searches

Neutral hydrogen absorbers

Diffuse polarization of the Galaxy

Instrumental approach:

1024 close-packed 6-m dishes

Dishes are stationary but can be tilted

Operating frequency: 400 – 800 MHz,
equivalent redshift = 0.8 – 2.5

Working closely with CHIME:
channelize with FPGA ICE boards,
correlation with GPUs

Location: SKA/Karoo (site agreement
in progress)

The acronym:



Rock hyrax / dassie



<http://www.acru.ukzn.ac.za/~hirax>

HIRAX: A Probe of Dark Energy and Radio Transients

L.B. Newburgh^a, K. Bandura^{b,c}, M. A. Bucher^{d,e}, T.-C. Chang^f, H.C. Chiang^{g,h}, J.F. Clicheⁱ,
 R. Dave^{j,k,l}, M. Dobbsⁱ, C. Clarkson^{m,n}, K. M. Ganga^d, T. Gogo^o, A. Gumba^o, N. Gupta^p, M.
 Hilton^h, B. Johnstone^{b,c}, A. Karastergiou^{q,r,s}, M. Kunz^t, D. Lokhorst^{a,u}, R. Maartens^q, S.
 Macpherson^o, M. Mdlalose^e, K. Moodley^h, L. Ngwenya^e, J.M. Parraⁱ, J. Peterson^v, O. Recnik^a,
 B. Saliwanchik^h, M. G. Santos^q, J.L. Sievers^{e,g}, O. Smirnov^s, P. Stronkhorst^w, R. Taylor^m, K.
 Vanderlinde^{a,u}, G. Van Vuuren^o, A. Weltman^{m,x,y}, and A. Witzemann^q

^aDunlap Institute, University of Toronto, 50 St. George St., Toronto, Canada

^bLane Department of Computer Science and Electrical Engineering, West Virginia University,
 PO Box 6201, Morgantown, WV 26506, USA

^cDepartment of Physics and Astronomy, West Virginia University, PO Box 6201, Morgantown,
 WV 26506, USA

^dAPC, Univ Paris Diderot, CNRS/IN2P3, CEA/lrfu, Obs de Paris, Sorbonne Paris Cité,
 France

^eAstrophysics & Cosmology Research Unit, School of Chemistry and Physics, University of
 KwaZulu-Natal, Durban, South Africa National Institute for Theoretical Physics,
 KwaZulu-Natal, South Africa

Required specs for BAO intensity mapping

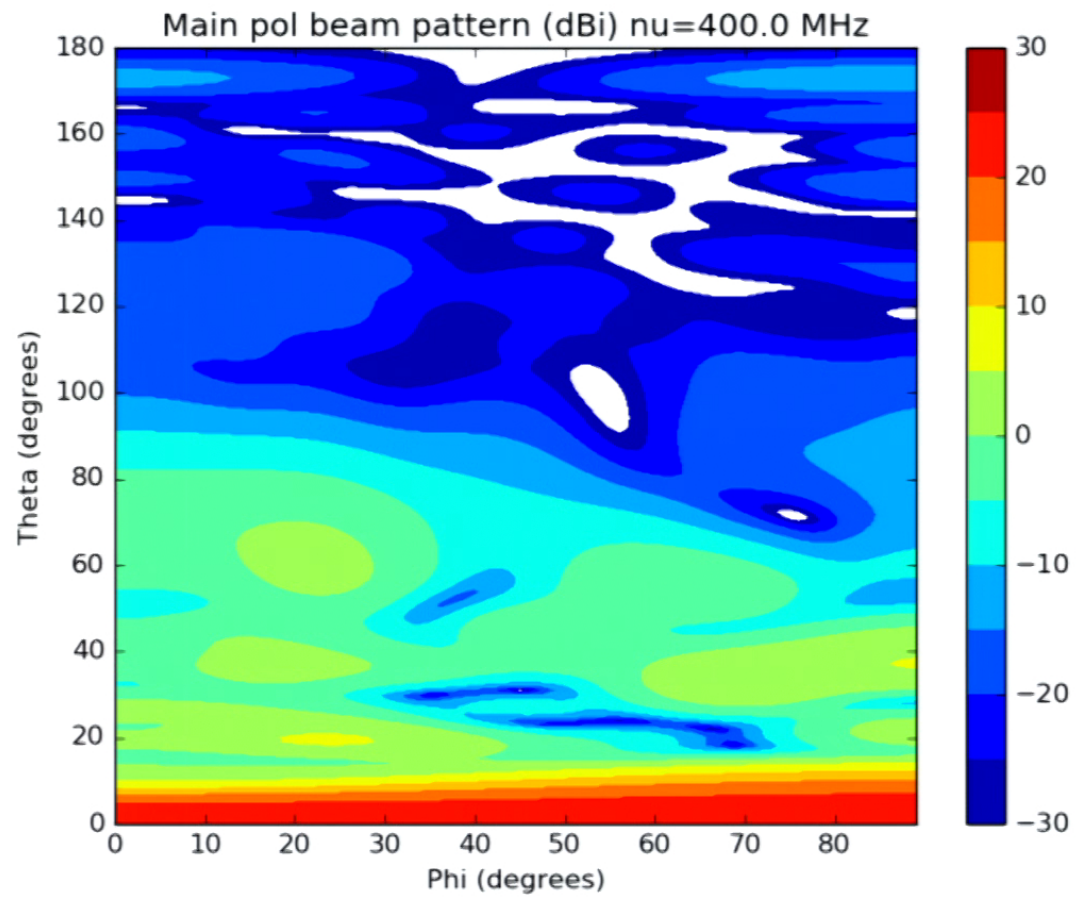


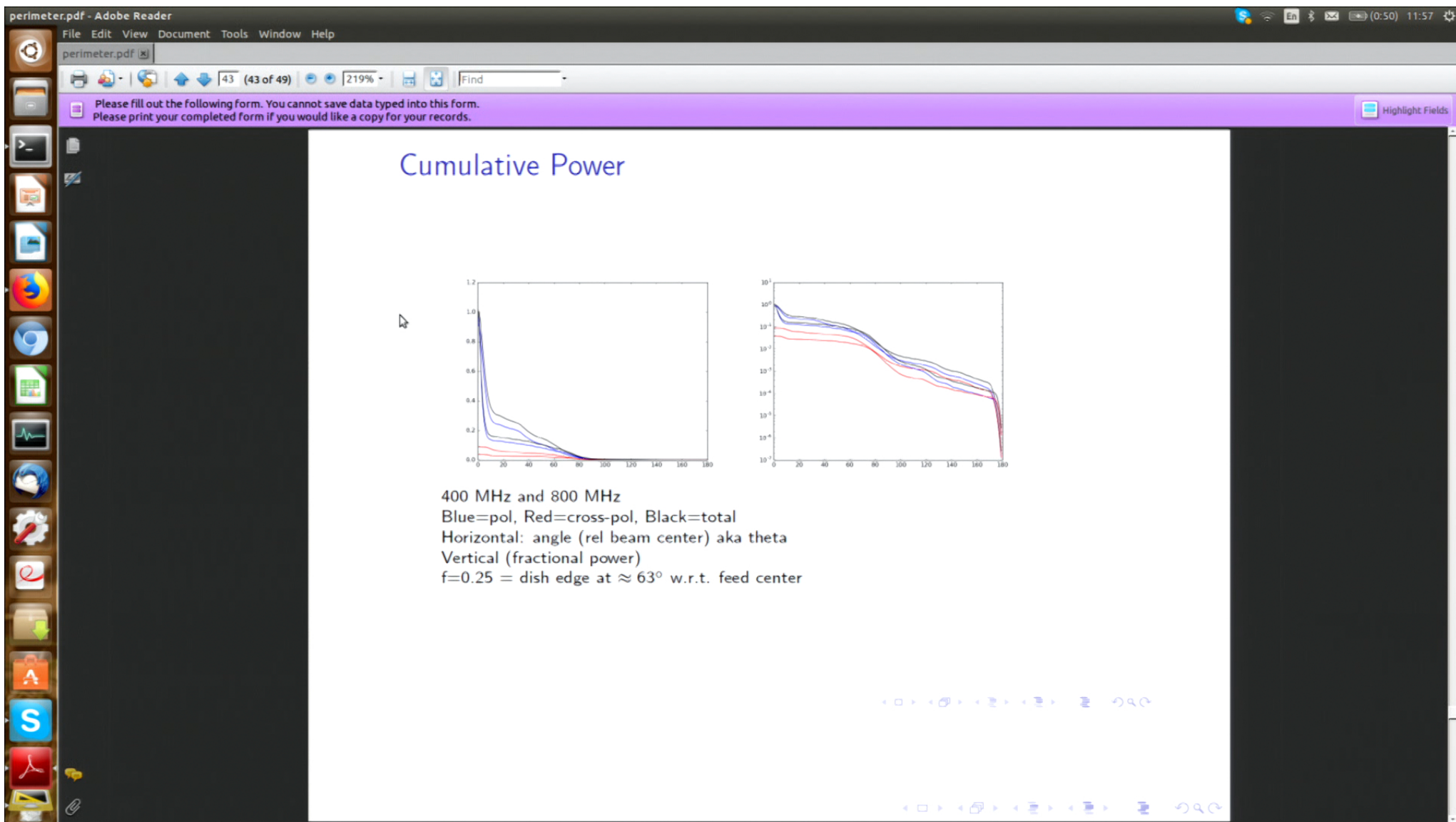
- Maximize sensitivity on scales of interest
→ Use compact array geometry
- Redshift range of interest: $0.8 < z < 2.5$ to capture dark energy domination at $z \sim 2$
→ Required frequencies: 400 – 800 MHz
- BAO 150 Mpc angular scale: 3 – 1.3 degrees at $0.8 < z < 2.5$
→ Required baseline lengths: 15 – 60 meters
- BAO scale along line of sight: 20 – 12 MHz at $0.8 < z < 2.5$
→ Required freq resolution: minimum ~100 channels, more for foregrounds and higher order peaks
- BAO signal level: ~0.1 mK
→ Low system temperature, large collecting area

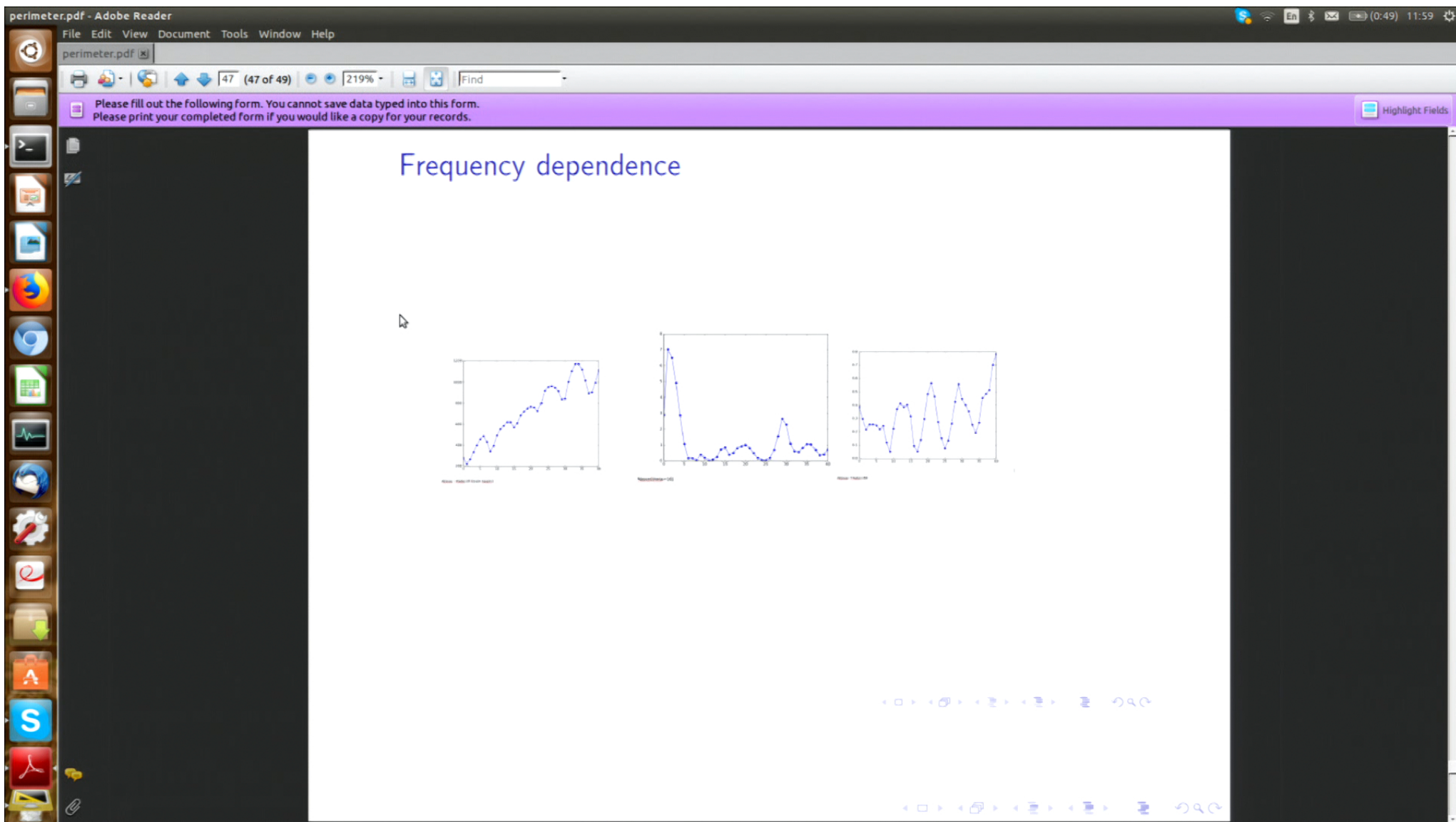
Navigation icons: back, forward, search, etc.

Navigation icons: back, forward, search, etc.

Main polarization







perimeter.pdf - Adobe Reader

File Edit View Document Tools Window Help

perimeter.pdf x

48 (48 of 49) 219% Find

Please fill out the following form. You cannot save data typed into this form. Please print your completed form if you would like a copy for your records. Highlight Fields

Oscillations from CHIME-(similar but different)

4.1 Single slice properties

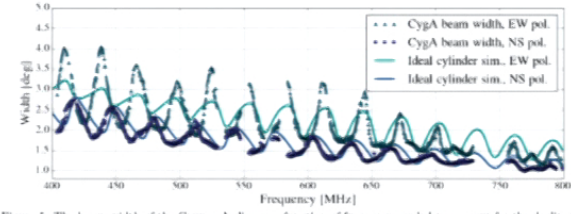


Figure 5: The beam width of the Cygnus A slice as a function of frequency, scaled to account for the declination of the source, for both polarisations of a single feed on the East cylinder. Also plotted are the predictions from numerical simulations of an ideal parabolic cylinder illuminated by a CHIME Pathfinder feed. The dominant mode of the oscillation has a period of ~ 30 MHz, matching the light travel time of twice the 5 m focal length of the Pathfinder. This is a well-known phenomenon in on-axis telescopes.^{26,27} See Figure 4 and also Ref. 17

From: Berger, Philippe; Newburgh, Bandura, et al., "Holographic beam mapping of the CHIME pathfinder array," Proceedings of the SPIE, Volume 9906, id. 99060D 16 pp. (2016) arXiv e-print (arXiv:1607.01473)